

# Heat transfer characteristics in centrifuge melt-spinning

J. BARAM

*Materials Engineering Department, Ben-Gurion University of the Negev, Beer-Sheva, Israel*

Centrifuge melt-spinning (CMS) is a new technique for the production of rapidly solidified metallic ribbons. In CMS, centrifugal forces are used twice: to eject the liquid melt on to the quenching substrate (a copper rim) by rotation of the casting crucible, and to ensure prolonged contact of the solidifying ribbon with the heat extraction sink by making the quenching rim rotate too, in the opposite direction. The heat transport in CMS has a Newtonian nature, as it can be considered as a constant-resistance heat transfer process. Calculated heat transfer coefficients  $h$  range between  $(1.55 \text{ to } 4.30) \times 10^{-6} \text{ W m}^{-2} \text{ sec}^{-1}$ , a half to one order of magnitude higher than for conventional melt-spinning. Increasing the ejection pressure from 1.8 to 269 kPa causes the apparent heat transfer coefficient to increase by a factor of three. Conversely to conventional melt-spinning, two additional phenomena contribute to the heat transfer characteristics in CMS at high extraction velocities: forced convection and mechanical dragging of the melt. The overall effect is a net improvement of the heat transfer ability in CMS as compared to conventional melt-spinning.

## 1. Introduction

Centrifuge melt-spinning (CMS) is a new technique for the production of rapidly solidified metallic ribbons [1–3]. In CMS, centrifugal forces are used twice: to eject the liquid melt on to the quenching substrate (a copper rim) by rotation of the casting crucible, and to ensure prolonged contact of the solidifying ribbon with the heat extraction sink by making the quenching rim rotate too, in the opposite direction. The ejection pressure of the melt can be varied, and practical extraction velocities can attain large values (up to  $100 \text{ m sec}^{-1}$ ). Measurements of secondary dendritic arm spacings in the rim-side surface of a centrifuge melt-spun Al–12 at % Ge alloy have shown that cooling rates as high as  $10^8 \text{ K sec}^{-1}$  have been achieved [1–3]. This is believed to be due to improved thermal contact of the molten alloy puddle to the cooling substrate, and to a beneficial combination of crucible and substrate velocities. In CMS, as well as in conventional melt-spinning, the processed liquid metal tends to wet the casting rim surface. The air boundary layer associated with the rotating of the rim does restrict the wetting somehow, and the rim-contact side of the solidified ribbons show therefore a “wetting pattern”, which provides information about the metal–rim interfacial characteristics [4]. The presence of air pockets, where good contact between metal and substrate is lacking, may impair the interfacial heat transfer. In CMS, however, the hydraulic behaviour of the liquid melt is complex [5]. The relatively large amount of kinetic energy of the impinging melt causes the thermal contact between the melt and the substrate to be significantly improved. It is therefore a matter of interest to evaluate the heat transfer coefficients

associated with the quenching process in CMS, when ejection pressures and extraction velocities are varied.

The present paper reports the results of an evaluation study of the heat transfer characteristics of the quenching mechanism in CMS.

## 2. Experimental procedure and results

The details of the experimental processing of the Al–12 at % Ge alloy ribbons by CMS have been extensively described elsewhere [1–4]. Ejection pressures ranged from 1.8 to 269 kPa (corresponding to the crucible rotating at linear velocities from 6.5 up to  $25 \text{ m sec}^{-1}$ ), and substrate velocities ranged from nil to  $78 \text{ m sec}^{-1}$ . Volumetric flow rates were from  $1.3$  up to  $5.0 \text{ cm}^3 \text{ sec}^{-1}$ . Ribbons were produced at various thicknesses (15 to  $87 \mu\text{m}$ ) and widths (0.93 to 3.23 mm). Secondary dendritic arm spacings (DAS) were measured, using scanning electron microscope (SEM) examination.

The solidification heat transfer process involved in CMS is considered, at a first approximation, as a solidification process with contact resistance. The temperature of the rim is assumed to remain constant. The temperature gradient within the solidifying ribbon, tenths of a micrometre thick, is small. The average heat transfer coefficient  $h$  at the metal–rim interface can then be evaluated, when the relation between ribbon thickness  $t$  and quenching time  $\theta$  is known. In CMS, hydraulic considerations [5] shown that the melt residence time (which is identical to the quenching time) is given by the relation

$$\theta = \frac{W - d_0}{2V_s} \quad (1)$$

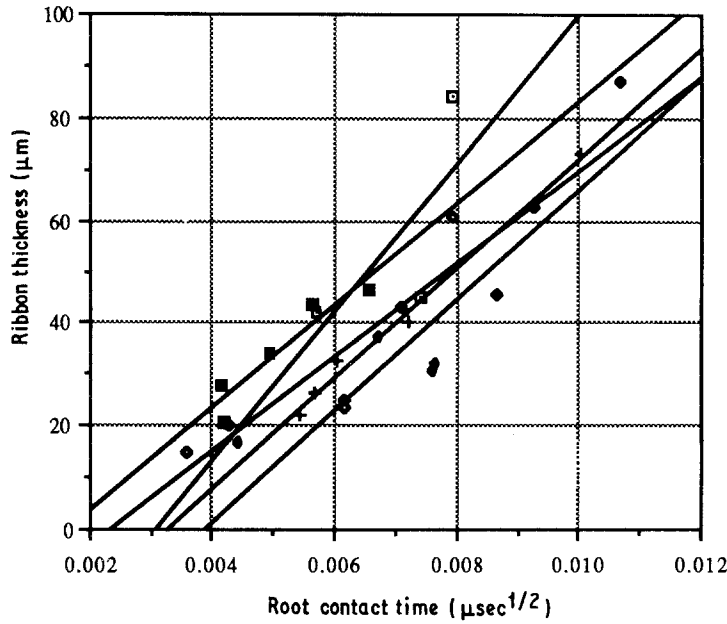


Figure 1 Ribbon thickness against the square root of melt residence time, for various ejection pressures. The linear best-fit equations are as follows for each curve; the free terms are the respective ordinate intercepts  $t_i$ . ( $\square$ )  $P_{ej} = 1.8$  kPa;  $y = -44.2031 + (1.443 \times 10^4)x$  ( $R = 0.72$ ). ( $\blacklozenge$ )  $P_{ej} = 20.4$  kPa;  $y = -41.8313 + (1.080 \times 10^4)x$  ( $R = 0.92$ ). ( $+$ )  $P_{ej} = 62.3$  kPa;  $y = -34.7212 + (1.069 \times 10^4)x$  ( $R = 1.00$ ). ( $\diamond$ )  $P_{ej} = 97$  kPa;  $y = -20.9803 + 9098.2326 x$  ( $R = 0.94$ ). ( $\blacksquare$ )  $P_{ej} = 269$  kPa;  $y = -15.9643 + 9945.0946x$  ( $R = 0.94$ ).

where  $W$  is the solid ribbon width,  $d_0$  is the diameter of the impacting liquid jet and  $V_s$  is the velocity of the liquid jet impacting on the rim. This relation holds as a first approximation, as  $V_s$  is calculated as the total (vectorial) contribution of the radial and tangential velocities of the ejected liquid stream and the additional velocity component imparted to the liquid by the centrifugal force of the rotating rim [5]. As the liquid jet spreads on the quenching rim, its thickness is reduced (until it solidifies), and the centrifugal force to which it is submitted decreases. The contribution of that additional velocity component to  $V_s$  is about 10% [5]. Assuming, as a first approximation, a constant  $V_s$ , leads therefore to a slight overestimation of  $\theta$ .

In Fig. 1, the linear best fits of the ribbon thickness against the square root of the melt residence time are depicted, together with the best-fit equations. The ordinate intercepts  $t_i$  of the empirical curves of  $t$  against  $\theta^{1/2}$  yield the average interfacial heat transfer coefficients  $h$  according to the relation [6]

$$h = -\kappa_s / 2t_i \left[ 1 + \left( \frac{\kappa_s \rho_s C_s}{\kappa_m \rho_m C_m} \right)^{1/2} \right] \quad (2)$$

where  $\kappa$  is the thermal conductivity,  $\rho$  is the density and  $C$  is the specific heat. The subscript  $s$  refers to the solid Al-Ge alloy at the solidifying temperature and the subscript  $m$  to the quenching substrate material (copper) at room temperature. The relevant material properties are listed in Table I, where the numerical values were calculated by appropriately weighting

aluminium and germanium data [7]; the subscript 1 refers to the liquid Al-Ge alloy at the superheat temperature. According to Southin and Chadwick [8], an undercooling of  $0.333 T_{\text{solidus}}$  for heterogeneous nucleation is assumed, i.e. the freezing temperature of the Al-12 at % Ge alloy is 582 K. The superheat used in practice was 150 K.

The average heat transfer coefficients calculated from Fig. 1 best-fits are tabulated in Table II.

Examination of Fig. 1 shows that none of the fitted straight lines  $t_i$  against  $\theta^{1/2}$  can be extrapolated to include the coordinate origin. This experimental observation justifies the contact-resistance heat transfer model, which means that cooling is essentially Newtonian, not ideal. The calculation of the  $h$  values shows that increasing the ejection pressure from 1.80 to 269 kPa causes the average heat transfer coefficient to increase almost three times, from  $1.56 \times 10^6$  to  $4.33 \times 10^6 \text{ W m}^{-2} \text{ K}^{-1}$ .

The magnitude of the mean cooling rate initially generated in the melt,  $\dot{T}$ , can now be estimated. For cooling via a heat transfer coefficient, i.e. Newtonian cooling, the following relationship holds [6]:

$$\dot{T} = \frac{Bi \kappa_1 \Delta T}{t^2 C_1} = \frac{h \Delta T}{t C_1} \quad (3)$$

where  $\Delta T$  is the temperature drop of the solidifying melt, namely 730 K, due to the fact that the alloy is submitted to a superheat of 150 K, and  $Bi$  is the Biot number. The measured and calculated results, for all

TABLE I Selected materials properties

Symbol	Property	Value
$\kappa_s$	Thermal conductivity of solid Al-12 at % Ge at 582 K	$192.6 \text{ W m}^{-1} \text{ K}^{-1}$
$\kappa_1$	Thermal conductivity of liquid Al-12 at % Ge at 1030 K	$75.6 \text{ W m}^{-1} \text{ K}^{-1}$
$\kappa_m$	Thermal conductivity of copper at 300 K	$397.0 \text{ W m}^{-1} \text{ K}^{-1}$
$\rho_s$	Density of solid Al-12 at % Ge at 582 K	$3360 \text{ kg m}^{-3}$
$\rho_1$	Density of liquid Al-12 at % Ge at 1030 K	$3196 \text{ kg m}^{-3}$
$\rho_m$	Density of copper at 300 K	$8920 \text{ kg m}^{-3}$
$C_s$	Specific heat of solid Al-12 at % Ge at 582 K	$2.895 \times 10^6 \text{ J m}^{-3} \text{ K}^{-1}$
$C_1$	Specific heat of liquid Al-12 at % Ge at 1030 K	$3.607 \times 10^6 \text{ J m}^{-3} \text{ K}^{-1}$
$C_m$	Specific heat of copper at 300 K	$3.434 \times 10^6 \text{ J m}^{-3} \text{ K}^{-1}$

TABLE II Average heat transfer coefficients at the practiced ejection pressures

Ejection pressure (kPa)	Heat transfer coefficient ( $\text{W m}^{-2} \text{K}^{-1}$ ) $\times 10^6$
1.80	1.56
20.40	1.65
62.30	1.99
97.00	3.30
269.00	4.33

ribbons where DAS measurements were performed, are given in Table III. The cooling rates developed on the rim-contact side of the ribbons have been calculated from the DAS measurements using the experimental relationship, for Al-Cu and Al-Si alloys [10]:

$$\lambda \varepsilon^{1/3} = 50 \mu\text{m} (\text{K sec}^{-1})^{1/3} \quad (4)$$

where  $\lambda$  is the measured DAS and  $\varepsilon$  is the cooling rate.

The various cooling rates experienced by the processed ribbons did yield spectacular changes in microstructure and occurrence of excess solubility of germanium in aluminium [11]. A detailed study of the microstructure evolution and its connection to process parameters is given elsewhere [12]. Fig. 2 shows how dendritic structure, for example, progressively disappears when the cooling rate is increased.

### 3. Discussion

CMS involves heat flow into a convex surface and is therefore divergent, whereas in conventional melt-spinning the heat flows convergently into a concave surface, and is therefore less rapid (see Fig. 3). This geometrical feature alone points towards some improvement in the heat transfer capability of CMS as compared to conventional melt-spinning. The additional beneficial effects produced by the peculiar process features of CMS, namely the centrifugal forces exerted on the melt and the high extraction

velocities, are clearly depicted in Table III. For a same ejection pressure, the higher the total (extraction) velocity, the higher the cooling rates. Moreover, when ribbons are compared that were obtained at the same extraction velocities, but at higher ejection pressures, the cooling rates increase again. The same trends are observed either when the initial mean cooling rates  $\bar{T}$  are involved or the DAS-derived cooling rates. The correlation between the two sets of calculated values is, however, somehow complex. At low ejection pressures (20.4 kPa), the cooling rates calculated from DAS are systematically higher (by a factor of 2 to 3) than those evaluated through the contact-resistance heat transfer model. At intermediate (97 kPa) and high (269 kPa) ejection pressures, the  $\bar{T}$  values are higher than the cooling rates calculated from DAS, for all ribbons but those few processed at very high extraction velocities (ribbon Nos 30, 20 and 29). The DAS measurements are a direct evidence of the microstructural features of the substrate side of the ribbons. Conversely,  $\bar{T}$  calculations are derived from the computed  $h$  values. These value may be well over or underestimated, if heat transport is affected by side effects, such as *forced convection* due to the peculiar hydraulic conditions of the liquid melt, or *dragging* due to the counter-rotation of the casting crucible and the quenching substrate. The effect of forced convection may be assessed for by taking higher values for  $\kappa_s$ , the thermal conductivity of the solid, and thus lowering the actual values of  $h$  and  $\bar{T}$ . The influence of this forced convection on the constitutional undercooling of the melt is discussed elsewhere [12]. The dragging phenomenon causes the thinning of the solidifying melt by a shear mechanism. As a result, momentum transport becomes effective, in addition to energy (heat) transport. Such an effect is particularly important as high extraction velocities are practiced. Its existence has indeed been deduced from a wetting pattern analysis performed on the CMS ribbons [4].

TABLE III Measured and calculated process values for Al-Ge centrifuge melt-spun ribbons

Specimen No.	$P_{ej}^\dagger$ (kPa)	DAS* ( $\mu\text{m}$ )	$V_{total}^*$ ( $\text{m sec}^{-1}$ )	Thickness* ( $\mu\text{m}$ )	Width* (mm)	Mean cooling rate $^\ddagger$ ( $\text{K sec}^{-1}$ ) $\times 10^7$	
						From $\bar{T}$	From DAS
1.	20.4	0.270	9.0	87.0	2.63	0.38	0.64
2.		0.255	14.8	45.4	1.88	0.74	0.75
3.		0.165	25.1	32.0	1.66	1.04	2.78
4.		0.160	33.1	30.6	1.68	1.09	3.05
5.		0.150	48.4	24.7	1.30	1.35	3.70
33.		0.145	87.9	16.7	0.93	2.00	4.10
10.	97.0	0.380	21.8	60.8	2.65	1.10	0.23
8.		0.350	32.1	43.2	2.25	1.55	0.29
7.		0.275	40.1	37.4	2.10	1.79	0.60
6.		0.255	55.4	23.5	1.88	2.84	0.75
28.		0.200	65.8	20.1	1.17	3.32	1.56
30.		0.110	95.9	15.0	0.98	4.45	9.40
15.	269.0	0.360	30.8	46.6	2.77	1.88	0.27
16.		0.315	41.1	43.7	2.22	2.00	0.40
25.		0.250	49.1	34.0	1.82	2.58	0.80
20.		0.130	64.4	27.8	1.45	3.15	5.69
29.		0.125	74.8	20.7	1.48	4.23	6.40

\* Experimental values,  $^\ddagger$  calculated values.

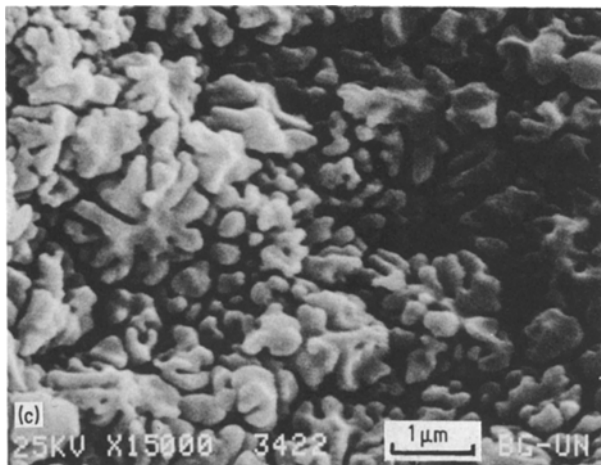
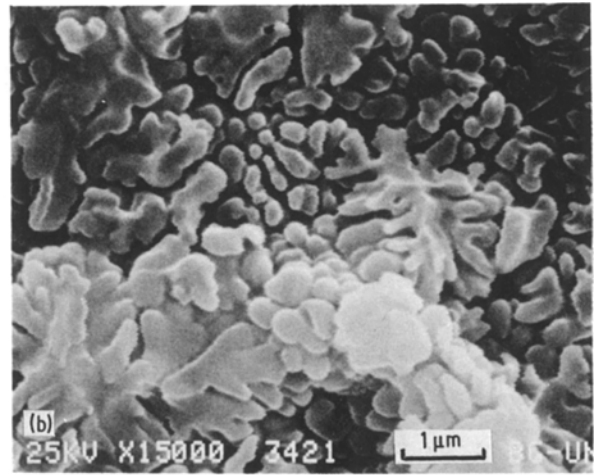
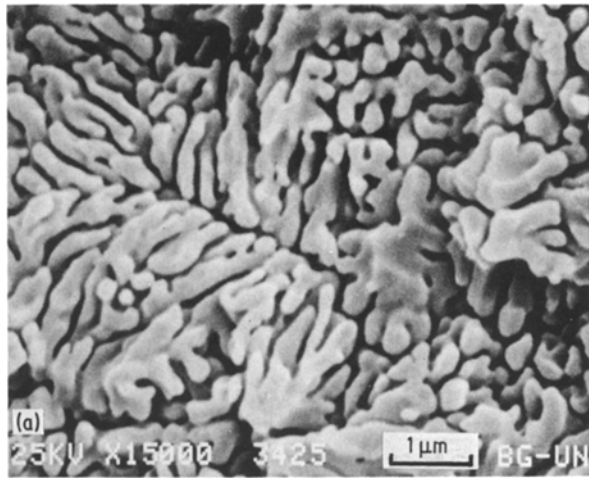


Figure 2 Disappearance of dendritic structure as cooling rate increases. (a) Ribbon No. 24,  $\dot{T} = 6.0 \times 10^6 \text{ K sec}^{-1}$ ; (b) Ribbon No. 7,  $\dot{T} = 17.9 \times 10^6 \text{ K sec}^{-1}$ ; (c) Ribbon No. 20,  $\dot{T} = 31.5 \times 10^6 \text{ K sec}^{-1}$ .

#### 4. Conclusions

The heat transport in CMS has a Newtonian nature, as it can be considered as a constant-resistance heat transfer process. Calculated heat transfer coefficients  $h$  range between  $(1.55 \text{ to } 4.30) \times 10^6 \text{ W m}^{-2} \text{ sec}^{-1}$ , a half to one order of magnitude higher than for conventional melt-spinning. The heat transfer characteristics of CMS show several advantages of this new technique over conventional melt-spinning. The divergent nature of the heat flow in CMS enables faster heat removal than the convergent geometry of conventional melt-spinning. The heat transport in CMS is directly affected by the increase of the centrifugal forces used to eject the liquid melt on to the quenching substrate and to ensure the prolonged contact of the solidifying ribbon with the heat extraction sink. Increasing ejection the pressure from 1.8 to 269 kPa causes the apparent heat transfer coefficient to increase by a factor of three. Conversely to conventional melt-spinning, two additional phenomena contribute to the heat transfer characteristics in CMS at high extraction velocities: forced convection and mechanical dragging of the melt. The forced convection phenomenon is

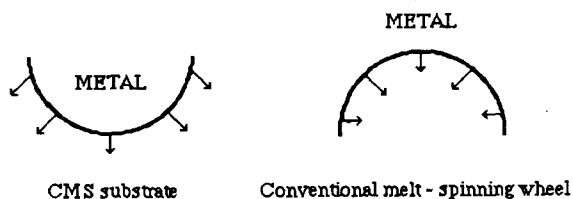


Figure 3 Effect of substrate contour on heat flow.

probably detrimental to the heat transfer ability of the system. However, at these high extraction velocities there is a mechanical dragging mechanism, due to the counter-rotation of the casting crucible and the quenching rim, which causes enhanced thinning of the melt prior to solidification. Momentum transport becomes effective in addition to energy (heat) transport. The overall effect is a net improvement of the heat transfer ability in CMS as compared with conventional melt-spinning. A detailed mathematical study of the combined momentum and heat transport in CMS is now in progress [5].

#### Acknowledgements

The experimental work that yielded the results on which this study is based (on the Al-12 at % Ge alloy) was performed as a partial requirement for the MSc degree in Materials Engineering by Mrs G. Rosen, at the Rapid Solidification Laboratory, Materials Engineering Department BGU.

#### References

1. G. ROSEN, J. AVISSAR, Y. GEFEN and J. BARAM, in "Rapidly Solidified Materials", Proceedings of an International Conference, San Diego, California, February 1986, edited by P. W. Lee and R. S. Carbonara (American Society for Metals, 1985) p. 9.
2. *Idem*, *J. Phys. D, Sci. Inst.* **20** (1987) 571.
3. *Idem*, *Int. J. Rapid Solidification* **2** (1986) 67.
4. J. BARAM, *J. Mater. Sci.* **23** (198) 405.
5. Z. RIVLIN, A. GRILL and J. BARAM to be published.
6. G. H. GEIGER and D. R. POIRIER, "Transport Phenomena in Metallurgy" (Addison-Wesley, Reading, Massachusetts, 1973) p. 346.
7. C. J. SMITHELLS (ed.), "Metals Reference Book", 5th Edn, (Butterworth, London, 1978).
8. R. T. SOUTHIN and G. A. CHADWICK, *Acta Metall.* **26** (1978) 223.
9. T. W. CLYNE, *Met Trans.* **15B** (1984) 369.
10. H. JONES, "Rapid Solidification of Metals and Alloys" (Institution of Metallurgists, London, 1982) p. 42.
11. G. ROSEN, MSc thesis, Ben-Gurion University (1986).
12. J. BARAM, to be published.

Received 9 January  
and accepted 1 April 1987